Transport of Carriers in Magnetic Brush Development Process of Electrophotography

Hiroyuki Kawamoto

Manufacturing Engineering Laboratory, Corporate Research Laboratories, Fuji Xerox Co., Ltd. 430 Sakai, Nakai-machi, Ashigarakami-gun, Kanagawa 259-01, Japan

A feasibility study has been performed to simulate the transport of magnetic carriers in a two-component magnetic brush development subsystem of electrophotography. A fundamental model has been established for the magnetic force, which acts on magnetic particles in the magnetic field applied by a magnetic roller. Numerical calculations have been conducted using a simplified model that neglects the interactive magnetic force between carrier particles. The qualitative adequacy of the model has been confirmed by comparing the calculated distribution of the magnetic force with the experimentally observed adherence mode of carrier beads on the magnetic roller. The present method can be utilized to support the design of magnetic brush development subsystems.

Journal of Imaging Science and Technology 40: 168 – 170 (1996)

Introduction

In an electrophotographic development subsystem, electrostatically charged toner particles are brought into the vicinity of an electrostatic latent image on a photoreceptor, and through the electric field created by the charges on the photoreceptor, the toner adheres to the latent image, transferring it to create a real image.[1] Although there are several types of development subsystems, such as cascade development, magnetic brush development, nonmagnetic monocomponent development, and liquid development, magnetic brush development is most widely used because it can readily produce a high level of copy quality.[1] However, because high performance is attained only when system parameters are optimized with respect to electrostatic and magnetic design conditions and the properties of the materials used in the system, many trial and error tests are normally required to determine the correct conditions. For this reason, many theoretical and experimental studies have been conducted on the topic of xerographic development process optimization. However, investigations with respect to magnetics are currently not well developed, so the design of a magnetic system, such as the magnetization profile of a magnetic roller, is not deductive but depends instead largely on prior empirical observations.

In this study, the author has investigated the transport of magnetic particles in a magnetic brush development subsystem and proposes a numerical method to support efficient design of the subsystem, in particular the design of the magnetic roller.

Magnetic Brush Development Subsystem in Electrophotography

A schematic drawing of a two-component magnetic brush development susbsystem is shown in Fig. 1. In this subsystem, the toner is electrostatically charged by mixing with carrier beads. The carrier beads are magnetically soft spheres coated with a polymer chosen to charge the toner on contact. By virtue of the magnetic properties of the carrier beads, the carrier beads with attached toners are transported around a rotatory nonmagnetic sleeve, which has a stationary magnetic roller within it. In the development zone or gap, the magnetic field induced by the magnetic roller causes carrier beads to form chains.[2] Toner particles contact the photoreceptor at the ends of the carrier bead chains, and transfer of toner from the carrier chains to the latent image on the photoreceptor forms a real image.[1]

Magnetic Force

It is essential to calculate the force $\mathbf{F}_j$ that acts on the carrier j in the magnetic field. The force is assumed to consist of the force due to the magnetic field at the j site induced by

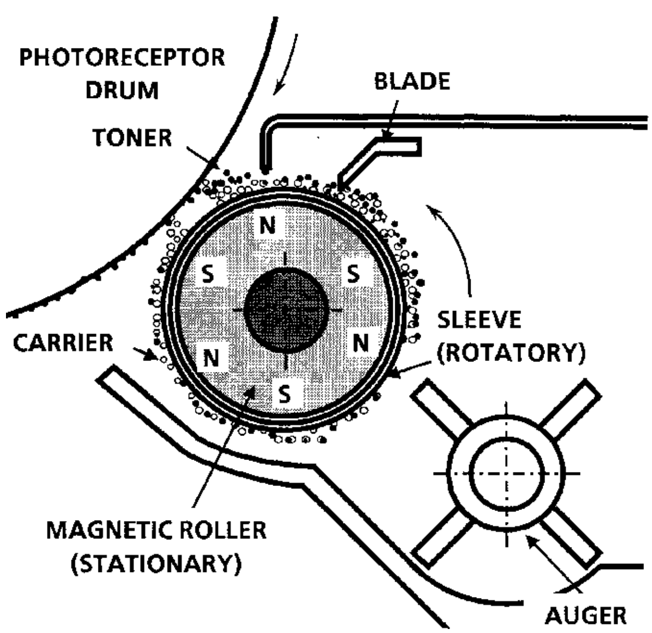

Figure 1. Schematic drawing of the two-component magnetic brush development subsystem.

Original manuscript received May 31, 1995.

the magnetic roller (the first term of the right side of Eq. 1) and the force due to the magnetic field at the j site induced by another carrier k (the second term of the right side of Eq. 1). Here the following assumptions are made: (1) The magnetized carrier does not change the magnetic field of the magnetic roller. (2) The magnetic flux density at a certain carrier site is affected by other carriers, but the magnetic dipole moment of the carrier is not affected by other carriers. (3) Forces except for magnetic ones, such as electrostatic, gravitational, and centrifugal forces, can be neglected. (Magnitudes of the neglected forces are estimated in the Appendix.) Thus, the force $\mathbf{F}_j$ can be given by:

$$\mathbf{F}_j = (\mathbf{m}_j \cdot \nabla)\mathbf{B}_j + \sum_{k=1\,(\neq j)}^{N} (\mathbf{m}_j \cdot \nabla)\mathbf{B}_{kj}, \tag{1}$$

where $\mathbf{m}_j$ is the magnetic dipole moment of carrier j, $\mathbf{B}_j$ is the magnetic flux density at carrier site j, and N is the total number of carriers. The magnetic dipole moment $\mathbf{m}_j$ and the magnetic flux density $\mathbf{B}_{kj}$ at the carrier site j due to another carrier k are expressed as follows:[2]

$$\mathbf{m}_j = \frac{4\pi}{\mu_0} \frac{\mu_j - 1}{\mu_j + 2} \frac{a_j^{\,3}}{8} \mathbf{B}_j \equiv \mathrm{C}_j \mathbf{B}_j, \tag{2}$$

$$\mathbf{B}_{kj} = \frac{\mu_0}{4\pi} \left[\frac{3(\mathbf{m}_k \bullet \mathbf{r}_{kj})}{r_{kj}^5} \mathbf{r}_{kj} - \frac{\mathbf{m}_k}{r_{kj}^3} \right], \tag{3}$$

where μ_0 is the permeability of free space, μ_j is the relative permeability of the carrier, a_j is the diameter of the carrier, $\mathbf{r}_{kj}$ is the position vector from the k-th to the j-th carrier, and r_{kj} is the absolute value of the vector $\mathbf{r}_{kj}$.

Because there are numerous carriers in the magnetic development subsystem, it is unrealistic and almost impossible to calculate numerically the second term of the right side of Eq. 1 over all of the carriers in the system. Therefore, the force due to the magnetic field induced by other carriers is neglected, i.e:

$$\mathbf{F}_j = (\mathbf{m}_j \cdot \nabla)\, \mathbf{B}_j = (\mathrm{C}_j\, \mathbf{B}_j \cdot \nabla)\, \mathbf{B}_j. \tag{4}$$

(The adequacy of this additional assumption is also discussed in the Appendix.) Equation 4 in coaxial cylindrical coordinates is:

$$F_{rj} = C_j \left(B_{rj} \frac{\partial B_{rj}}{\partial r} + \frac{\partial B_{\theta j}}{r} \frac{\partial B_{rj}}{\partial \theta} \right), \tag{5}$$

$$F_{\theta j} = C_j \left(B_{rj} \frac{\partial B_{\theta j}}{\partial r} + \frac{B_{\theta j}}{r} \frac{\partial B_{\theta j}}{\partial \theta} \right), \tag{6}$$

or

$$F_{rj} = C_j \left(-\frac{B_{rj}^{\;2}}{r} - \frac{B_{rj}}{r} \frac{\partial B_{\theta j}}{\partial \theta} + \frac{B_{\theta j}}{r} \frac{\partial B_{rj}}{\partial \theta} \right), \tag{7}$$

$$F_{\theta j} = C_j \left(-\frac{B_{rj} B_{\theta j}}{r} - B_{\theta j} \frac{\partial B_{rj}}{\partial r} + B_{rj} \frac{\partial B_{\theta j}}{\partial r} \right). \tag{8}$$

If the distribution of the magnetic flux density induced by the magnetic roller can be determined, then the magnetic

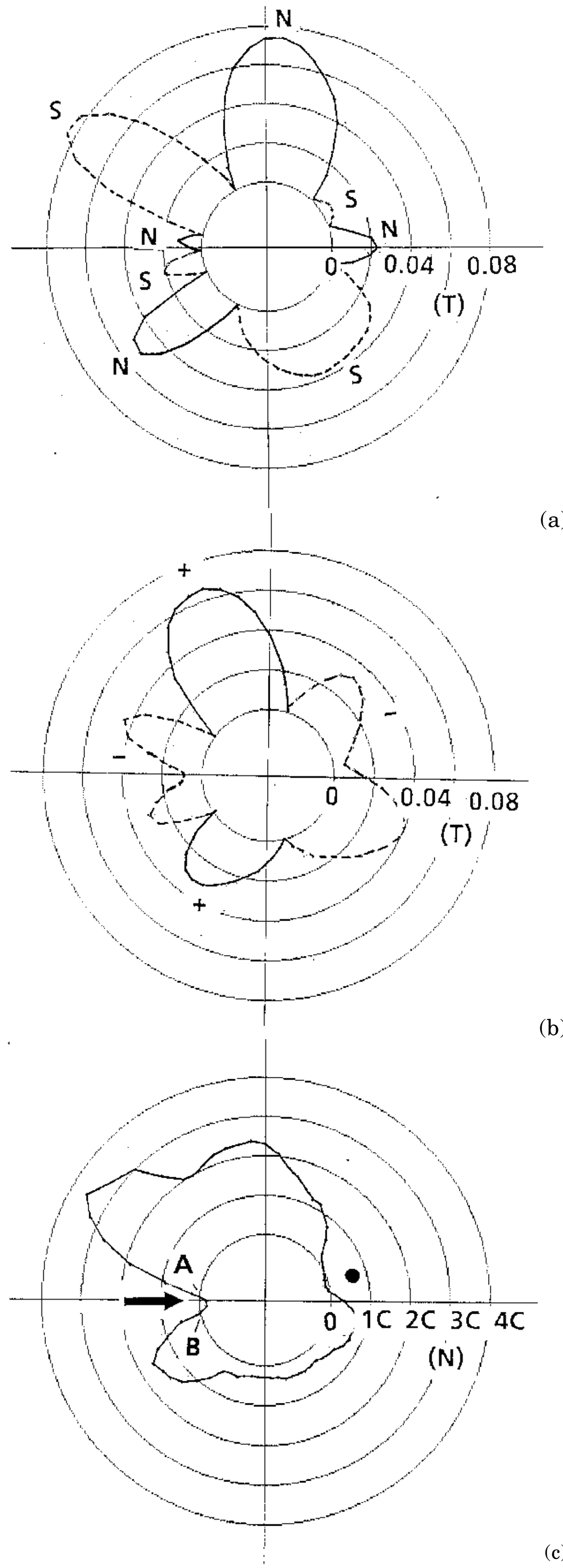

Figure 2. (a) Measured distribution of the radial magnetic flux density B_r at the sleeve surface and (b) circumferential magnetic flux density $B\theta$ at the sleeve surface. (c) Calculated distribution of the radial magnetic force, $-F_r$, to the carrier. Carriers are repulsed at the arrow region facing the photoreceptor. (T) in (a) and (b) is a unit of magnetic flux density, Tesla; (N) in (c) is a unit of force, Newton.

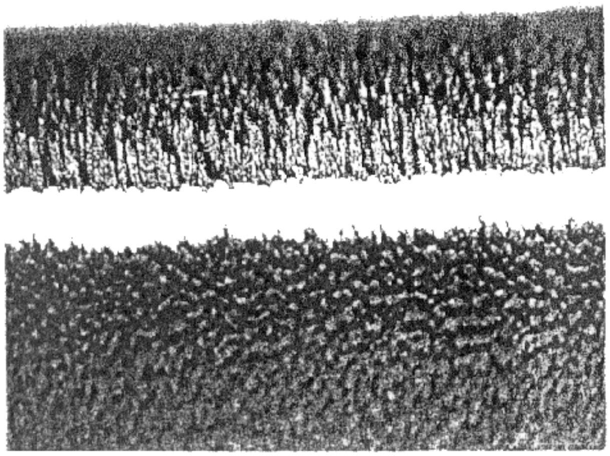

Figure 3. Magnetically adherent carriers at the sleeve surface. Carriers are repulsed in the white region, which is designed to face the photoreceptor.

force to the carrier can be calculated, using Eqs. 5 and 6 or Eqs. 7 and 8. Here it should be mentioned that both the magnetic flux density at a certain position and its gradient are required for the magnetic force calculation.

Results and Discussion

The relationship between the force calculated by the present simplified model and the transport characteristics of the carrier beads can be assessed from a comparison of the distribution of the calculated magnetic force and the experimentally observed mode of the carrier bead transport on the sleeve. Figures 2(a) and 2(b) show the distributions of the radial and circumferential magnetic flux densities, respectively, measured on the surface of a sleeve 24.5 mm in diameter, using a Hall probe. (In the actual design procedure, a numerically calculated magnetic flux density around the sleeve is used in place of the measured values. Details of the method to calculate the magnetic flux density have been reported in Ref. 3). With the distribution of the magnetic flux density input into Eq. 7, the radial magnetic force on the carrier can be calculated. Figure 2(c) shows the result.

Two interesting features can be deduced from Fig. 2. One is that the magnetic roller is designed so that the radial force is negative where it faces the development zone (marked by an arrow in the figure). This result means that a repulsive force acts on the carrier when the carrier is transported to part A, so that the carrier jumps to B in Fig. 2(c). This pattern coincides with the experimental observation shown in Fig. 3. In this arrangement, carrier chains do not directly touch the photoreceptor—only the jumping carrier beads contact the photoreceptor, and this eliminates the streaked image defect typically created by passage of carrier bead chains across a developed image. Another feature is that a similar repulsive region exists on the opposite side of the development zone [the bullet-marked region in Fig. 2 (c)]. This repulsive region facilitates the retoning process for the development brush. For example, if the carriers tightly adhere to the sleeve, then toner resupply to the development brush will be limited, and toner in the brush will be increasingly depleted by the development process. However, if the carriers separate from the sleeve in this low-force region, then carriers mixed with fresh toner can be supplied to the development sleeve. Although it is difficult to deduce by trial and error the optimized conditions for image development and toner replenishment, the present method can provide an analytical procedure for magnetic force optimization and design of the magnetic roller.

Conclusion

A fundamental model has been established for the magnetic force that acts on magnetic particles in a magnetic field applied by a magnetic roller, to simulate the transport of magnetic carriers in a two-component magnetic brush development subsystem of electrophotography. Although the model is based on simplified assumptions (e.g., the interactive magnetic force between carriers and electrostatic and mechanical forces is neglected), the qualitative adequacy of the model has been confirmed by comparing the calculated distribution of the magnetic force with the experimentally observed adhering modes of carriers on a test magnetic roller. Accordingly, the method can be utilized to support the design of magnetic development subsystems.

Acknowledgment. The author wishes to thank T. Aoshima for helpful suggestions and for the experimental data shown in Fig. 2. Figures 2 and 3 are reproduced from the Proceedings listed in Ref. 4. The author wishes to acknowledge the Japan Society of Mechanical Engineers for permission to reprint this material.

Nomenclature

a	=	diameter of carrier	m
$\mathbf{B}$	=	magnetic flux density ($\equiv B_r\mathbf{i} + B_\theta\mathbf{j}$)	T
$\mathbf{F}$	=	magnetic force on carrier ($\equiv F_r\mathbf{i} + F_\theta\mathbf{j}$)	N
$\mathbf{i}, \mathbf{j}$	=	unit vectors to r and θ coordinates	—
$\mathbf{m}$	=	magnetic dipole moment of carrier	Am^2
N	=	total number of carriers	—
$\mathbf{r}_{kj}$	=	position vector from k-th to j-th carrier	m
r_{kj}	=	absolute value of vector $\mathbf{r}_{kj}$	m
(r, θ)	=	coaxial cylindrical coordinates	m, rad
μ_0	=	permeability of free space	$4\pi \times 10^{-7}$ H/m
μ	=	relative permeability of carrier	—

Appendix

Interactive Magnetic Force between Carriers. The relative magnitude of the interactive magnetic force between carriers can be estimated by comparing the norm of the first and second terms of Eq. 1:

$$\frac{\left\|(\mathbf{m}_1 \cdot \nabla)\mathbf{B}_{12}\right\|}{\left\|(\mathbf{m}_1 \cdot \nabla)\mathbf{B}_1\right\|} \leq \frac{1}{4}\frac{\mu - 1}{\mu + 2} < 0.25.$$

The interactive magnetic force plays an important role in determining the microscopic shape of the carrier chain,[2] but it exerts a minor influence on the macroscopic mode of carrier adhesion.

Centrifugal Force. The ratio of the centrifugal force to the magnetic force is of the order of 10^{-2} in the typical case, $a = 55\ \mu m$, density of carrier = 2.3×10^3 kg/m^3, diameter of sleeve = 24.5 mm, and process speed = 0.13 m/s.

Gravitational Force. The ratio of the gravitational force to the magnetic force is of the order of 0.1 under the same conditions as cited above. Experimental observations confirm that the centrifugal and gravitational forces are negligible compared with the magnetic force.

References

1. L. B. Schein, *Electrophotography and Development Physics*, Springer-Verlag, New York, 1988.
2. R. S. Paranjpe and H. G. Elrod, *J. Appl. Phys.* **60** (1): 418 (1986).
3. H. Kawamoto, S. Serizawa, and F. Takei, *Fuji Xerox Technical Report,* No. **9**, 54 (1994) (in Japanese).
4. H. Kawamoto, *Proc. Volume of the D&D '94*, D628, 297 (1994) (in Japanese).